

Image Processing Techniques for Digital Orthophotoquad Production

Joy Hood

TGS Technology, Inc., Science and Applications Branch, EROS Data Center, Sioux Falls, SD 57198

Lyman Ladner and Richard Champion

U.S. Geological Survey, 345 Middlefield Road, Menlo Park, CA 94025

ABSTRACT: Orthophotographs have long been recognized for their value as supplements or alternatives to standard maps. Recent trends toward digital cartography have resulted in efforts by the U.S. Geological Survey to develop a digital orthophotoquad production system. Digital image files were created by scanning color infrared photographs on a microdensitometer. Rectification techniques were applied to remove tile and relief displacement, thereby creating digital orthophotos. Image mosaicking software was then used to join the rectified images, producing digital orthophotos in quadrangle format.

INTRODUCTION

ORTHOPHTOGRAPHS have long been recognized for their value as supplements or alternatives to standard maps. The U.S. Geological Survey (USGS) produces orthophotographs in quadrangle format from a variety of orthophoto instruments, all of which differentially transform a central perspective photograph to an orthogonal projection. With such instruments, scale correction is achieved by adjusting the optical magnification, and direction correction is achieved by image rotation with Dove prisms.

While these techniques produce orthophotographs of high quality, their applications are limited by their photographic form. Recent trends toward digital cartography have resulted in efforts to develop a digital orthophotoquad production system.

Digitizing an aerial photograph produces a digital file that represents the gray scale values of a scanned image. Rectification techniques applied to the digital image remove tilt and relief displacement, producing a digital orthophoto. A valuable aspect of a digital orthophoto is that image processing techniques, such as digital mosaicking, image enhancement, and data merging, can be applied. A number of experimental digital orthophotos for a variety of applications were produced from photographs of various scales. Final digital orthophoto products include

Fontana, CA	1:12,000	(mosaic)
Orchards, OR	1:4,800	
Orchards, OR	1:6,000	
Portland, OR	1:12,000	(mosaic)
McCall, ID	1:24,000	(mosaic)
Dane County, WI	1:12,000	(thirty-six quarter quadrangles)

The Fontana, Orchards, and Portland orthophotos were produced as part of an experimental multipurpose cadastre project. Final products included political boundaries, contours lines, place names, and land-use indicators either photographically embedded in the images or displayed as overlays. The McCall orthophoto was made from 1:80,000-scale National High Altitude Photography (NHAP) color infrared photography, and the Dane County products were produced from 1:40,000-scale color infrared photography.

PREVIOUS RESEARCH

The idea of a digital orthophoto is not new. Some of the mathematical models for restitution of scanner and scanned im-

ages were described by Konecny (1976). Horton (1978) described a method for generating digital orthophotos through a hardware approach that made use of an image dissector tube to scan imagery nonorthogonally. Keating and Boston (1979) explained a software system to create an orthophoto from digital elevation models (DEM) and imagery scanned on a microdensitometer (an instrument that converts image density at any location to digital form). By 1979, Konecny (1979) was able to summarize experiences with digital image rectification software and display photographs of his results. His strategy acknowledged the significance of DEM resolution to the rectification problem and suggested one transformation for DEM cells and a simpler bilinear transformation for picture elements (pixels) within a cell. The present work builds upon that strategy.

DIGITAL RECTIFICATION

The rectification software was developed along the lines proposed by Keating and Boston (1979) and Olsen (1984). The two main sources of input data are a digitized aerial photograph and a DEM. The raster file results from scanning the photograph to be rectified on an Optronics C-4500 drum film scanner.* The data of a standard 7.5-minute DEM have the following characteristics: (a) they consist of a regular array of elevations referenced in the Universal Transverse Mercator (UTM) coordinate system, (b) they are ordered from south to north in profiles that are ordered from west to east, and (c) they are stored as profiles in which the spacing of the elevations along and between each profile is 30 m (Figure 1).

In addition to the two main sources of information, several other data files are required. These files consist of ground coordinates of passpoints, photo coordinates of passpoints, camera calibration parameters, and photograph fiducial coordinates in the raster image system.

Initial input to the rectification process consisted of camera calibration parameters, ground coordinates, and photo coordinates of at least three passpoints of the photographs rectified. The exterior orientation of the photographs was solved using the familiar space resection (collinearity) equations (Wolf, 1974) (eq. 1). The six unknown orientation parameters (X_0 , Y_0 , Z_0 , ω ,

* Any use of trade, product, or firm names in this publication is for descriptive purposes only and does not imply endorsement by the U.S. Government.

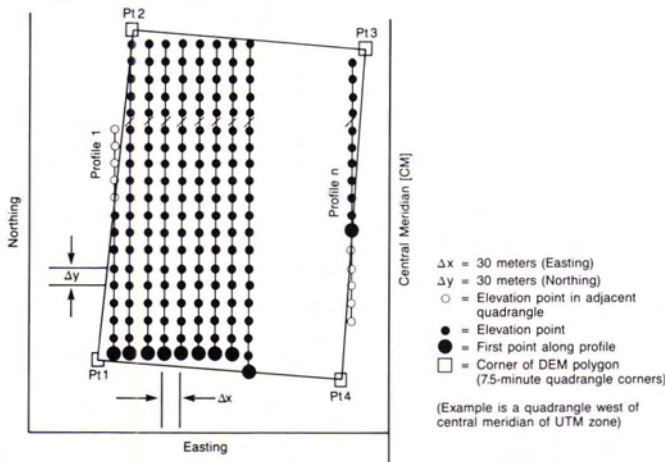


Fig. 1. Structure of a 7.5-minute digital elevation model.

ϕ, κ) were determined by the solution of the following equation for the photograph passpoints:

$$\begin{aligned}
 x &= -f * \frac{m_{11}(X_p - X_o) + m_{12}(Y_p - Y_o) + m_{13}(Z_p - Z_o)}{m_{31}(X_p - X_o) + m_{32}(Y_p - Y_o) + m_{33}(Z_p - Z_o)} \\
 y &= -f * \frac{m_{21}(X_p - X_o) + m_{22}(Y_p - Y_o) + m_{23}(Z_p - Z_o)}{m_{31}(X_p - X_o) + m_{32}(Y_p - Y_o) + m_{33}(Z_p - Z_o)}
 \end{aligned}
 \tag{1}$$

where

x, y are photo coordinates in the fiducial system;

X_p, Y_p, Z_p are passpoint ground coordinates;

X_o, Y_o, Z_o are camera station coordinates in ground system;

$m_{11}, m_{12}, \dots, m_{33}$ are rotation matrix elements which are functions of $\omega, \phi,$ and κ ; and

f is the known camera focal length.

The coordinates (lines and samples) of the fiducials in the raster image were determined. These coordinates were found by measuring their location on an image display device. (This step is not necessary if the scanner is registered to the fiducials.)

The photo coordinates were referenced to the camera fiducial coordinate system using the linear conformal transformation.

$$\begin{aligned}
 x_c &= ax_r - by_r + c \\
 y_c &= bx_r + ay_r + d
 \end{aligned}
 \tag{2}$$

where

x_c, y_c are calibrated fiducial coordinates;

x_r, y_r are fiducial coordinates in the raster image (line and sample); and

a, b, c, d are linear transformation parameters.

The first two profiles of the DEM were input to form a profile pair of DEM cells. The photo coordinates of the corners of each DEM cell in the profile pair were calculated using the previously determined parameters of exterior orientation. This calculation determined the number of lines of image data that were required to rectify the area between profiles.

The microdensitometer coordinates of the cell corners were computed using the photo coordinates, the linear transformation parameters, and the linear conformal transformation equations. This step was completed for each DEM cell in the profile pair. The required number of lines of image data were then read into computer memory.

The cell was partitioned to the desired resolution. For a res-

olution of 2 m on the ground, the 30-m DEM cell was divided into 15 by 15 or 225 subdivisions. For NAPP imagery at 1:40,000 scale, this gives a pixel size of 50 micrometres.

The elevation of a subdivision was calculated from the surrounding area using bilinear interpolation. After interpolation, the collinearity equations were again used with the previously calculated orientation parameters, and the easting and northing of the ground point within the DEM cell were determined to compute the photo coordinates of the subdivision. Photo coordinates were computed in this manner for each subdivision within the DEM cell.

The photo coordinates were referenced to the camera fiducial coordinate system so that the linear transformation parameters used to compute the line and sample of the raster image correspond to the photo coordinate. For each cell subdivision the 8-bit binary gray scale value that corresponds to the image coordinate was assigned to the subdivision image coordinate. Choosing a gray scale value to be moved from the input image file to the output image file was accomplished by image resampling. Currently, both nearest-neighbor resampling (using integer truncation to select the pixel) and cubic-convolution resampling (using a weighted average of neighboring pixels) are available.

The accuracy of the rectification process was measured by ascertaining the pixel coordinates of the passpoints appearing on the digital image and transforming them to their known positions. The passpoint locations in the orthophoto image were measured on a comparator, or image display device, and transformed to ground coordinates. The accuracy of the rectification was determined by comparing these measurements. Table 1 shows the result of a least-squares fit of 33 test points measured for the McCall, Idaho, digital orthophotoquad. The overall vector residual error was found to be 3.895 m, well within the map accuracy requirements for 1:24,000-scale mapping.

DIGITAL MOSAICKING OF ORTHOPHOTOS

Aerial photographs acquired under the NAPP are quarterquad centered. To produce a digital orthophotoquad complementing the 1:24,000-scale map series, digital mosaicking techniques must be used to join the digital orthophotos. This process removes the geometric and brightness discontinuities along mosaic seams. Because the images have been geometrically rectified to the desired map projection, the goal of the mosaicking process is to retain the geometric accuracy obtained during rectification while removing the small, but esthetically objectionable, discontinuities along the mosaic seams.

Four basic concepts were involved in the development of the Large Area Mosaicking System (LAMS). The first concept involves the use of carefully defined polygons inside the border of each image. These polygons define the location of the mosaic seams, determine where the automatic correlation routine is applied to produce seam control points (points for which line and sample coordinates are known in adjacent images), and limit processing to the portion of the scene included in the mosaic space. The second concept involves the adjustment of seam control points according to geographic control. Geographic control consists of points for which both the image line and sample and the geographic coordinates are known. The third concept involves the use of a compound geometric distortion model that corrects for lower spatial frequency distortions represented in the geographic control points, as well as the higher spatial frequency distortions represented by the seam control points. The fourth concept involves obtaining brightness correction information from the seam control points for use in adjusting brightness differences between adjacent images (Zobrist *et al.*, 1983). Another very important aspect of LAMS is the use of a data base system to manage the large amounts of tabular data generated in support of digital mosaicking. Digital

TABLE 1. MCCALL, IDAHO, DIGITAL ORTHOPHOTO TEST POINT MEASUREMENTS

Point Number	Vector Error		
	VE	VN	$\sqrt{VE^2 + VN^2}$
1	0.043	-3.798	3.798
2	-5.816	0.521	5.840
3	3.124	-0.494	3.161
4	0.262	-4.398	4.404
5	-1.484	-1.932	2.435
6	3.042	-2.451	3.908
7	3.557	-4.072	5.407
8	-2.868	-0.878	2.999
9	-4.532	-1.116	4.666
10	-2.679	-0.259	2.691
11	-1.106	0.283	1.143
12	-3.060	1.481	3.402
13	1.490	-0.253	1.512
14	1.695	-0.597	1.798
15	-0.061	3.527	3.527
16	-0.817	0.649	1.042
17	0.966	1.829	2.067
18	2.783	0.128	2.786
19	5.736	-1.807	6.014
20	4.615	0.704	4.670
21	-2.908	3.063	4.225
22	-0.704	2.551	2.646
23	-2.063	1.308	2.444
24	-0.878	2.079	2.164
25	-7.806	3.990	8.775
26	-5.206	3.880	6.492
27	-2.292	0.500	2.347
28	0.856	-1.734	1.939
29	2.731	4.054	4.889
30	-0.256	-1.439	1.460
31	1.923	-4.310	4.718
32	3.210	-1.878	3.719
33	0.287	-2.454	2.472
RMSE (Metres)	3.078	2.387	3.895

mosaicking is divided into two general processes — the geometric correction process and the radiometric or brightness correction process.

GEOMETRIC CORRECTION OF RECTIFIED AERIAL PHOTOGRAPHS

The first step in preparing a digital mosaic involves the selection of geographic control points. Because the individual digital orthophotos were geometrically rectified, the geographic control points are represented by a set of interior points used to hold the internal geometry of the images constant while removing the higher frequency geometric discontinuities along the mosaic seams. The passpoints used in the rectification process were used for geographic control points because they were well distributed throughout the images, and geographic and image coordinates were known.

The second step in the geometric correction process involves the selection of the polygonal boundaries for each image. As stated earlier, the polygons determine the location of the mosaic seams and seam control points while limiting processing to the portion of each image to be included in the final mosaic. The polygonal boundaries were manually selected using an image display device.

When working with digitally rectified aerial photographs, the selection of the polygonal boundaries is complicated by the spatial resolution of the data and the effects of look-angle. The polygons must be selected in such a way as to ensure that the effects of look-angle are minimized. For example, the polygon should not be selected through an area that is heavily shadowed in one

image and not in the other. Figure 2 shows a subsection of the polygon selected for orthophoto 241 of the Portland, Oregon mosaic and the corresponding area of the adjacent orthophoto image.

Seam control points are located by applying a fast fourier transform (FFT) phase correlation along the polygonal boundaries. The correlation involves extracting image windows about the predicted seam control point from each image and running a phase correlation on the two image windows. The seam control point location in the second image is gradually changed until the best correlation value is found. To avoid false correlations, care must be taken in the selection of the correlation window sizes. The spatial resolution of the digitally rectified Portland photograph, shown in Figure 2, is approximately 1 m. Periodic features (more than one road intersection) frequently occur if the correlation windows are too large. For each successful correlation, the line and sample locations for both images and the correlation values are stored in the respective control point files.

The seam control points are edited on the basis of a first-order fit of all points for a common overlap area (seam control for image one and two are edited separately from seam control for image one and four). The magnitude of the acceptable residuals is based on the geometric accuracy of the digital orthophoto images as measured by the passpoints. In the case of the Portland mosaic, residual errors as high as 4 pixels (4 m) were accepted.

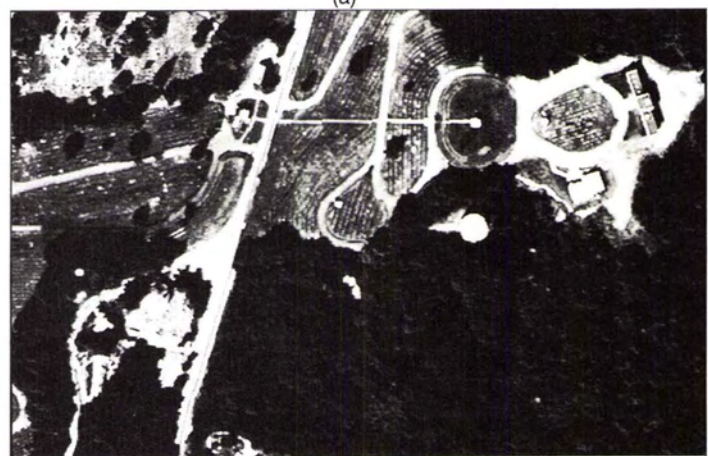
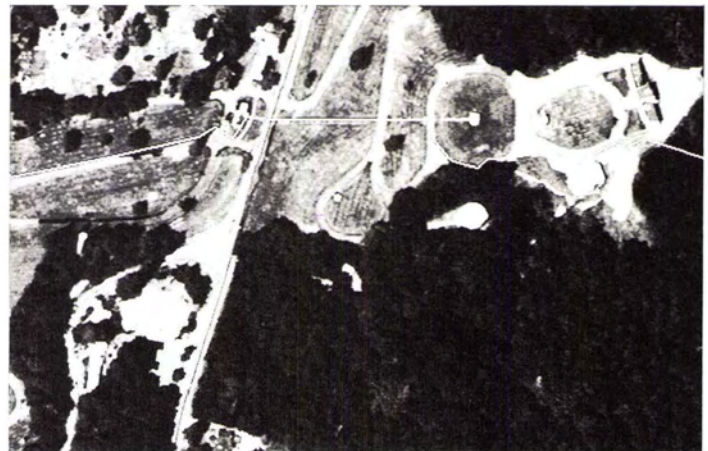


FIG. 2. Subsection of the polygonal boundary selected for photo 241.

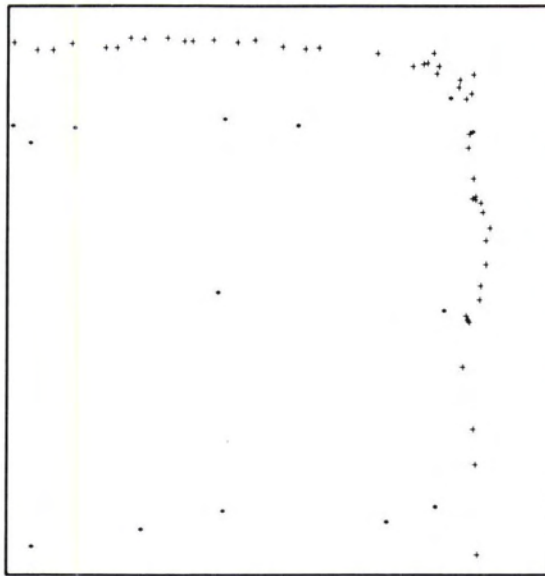
After editing, the seam control points are adjusted to ensure an identical mapping to output line and sample in adjacent images. The adjustment process reconciles the differences in mapped line and sample of the seam control points by averaging. The geometric correction model for each image is based on the geographic and the seam control points.

Most geometric correction models designed for rectifying image data make use of polynomials or satellite spacecraft and sensor models, which are adequate for correcting single image distortions. When rectification is used to mosaic adjacent images, a surface interpolation method that is continuous, yet can respond to the higher frequency distortions represented by the dense collection of seam control points, is required (Thormodsgard and Lillesand, 1987). The LAMS incorporates a triangulation

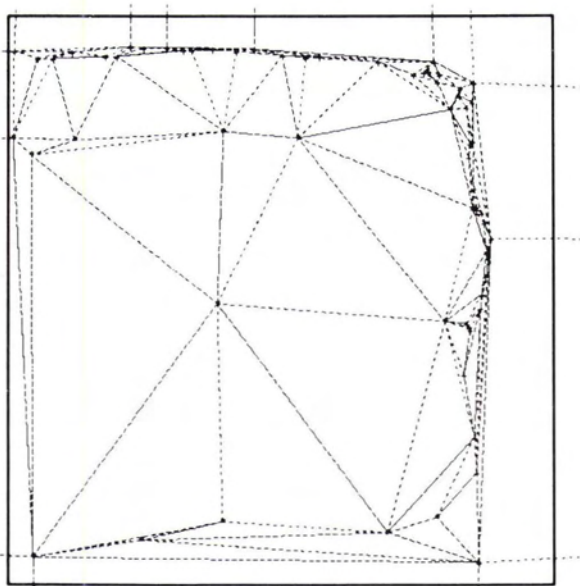
TABLE 2. PHOTO 14 PASSPOINT LOCATIONS AFTER RECTIFICATION AND MOSAICKING

Point Number	Predicted		After Rectification		After Transformation	
	Line	Sample	Line	Sample	Line	Sample
10030	160	158	160	165	157	159
10032*	1959	526				
10033	2079	180	2079	183	2079	182
10040*	168	158	167	1967		
10042	1941	2295	1940	2297	1939	2296
10050	467	3844	470	3846	469	3847
10052	1990	3673	1993	3676	1994	3678
10401*	1733	3500				
10411*	1894	1707				
10421*	1946	41				

* Point was unidentifiable due to image resampling.



(a)



(b)

FIG. 3. (a) Geometric and seam control for photo 241. (b) Faceted surface resulting from triangulation of geometric and seam control points.

technique developed by Manacher and Zobrist (1978) to combine the internal geographic control points and the seam control points in the creation of the surface interpolation model, known as the finite element technique. Zobrist and Manacher made use of the "greedy" triangulation technique in which edges are added to the triangular network based on their length. After ordering the edges from shortest to longest, edges are added to the triangulation network so long as they do not intersect existing edges in the network. Figure 3a illustrates geometric and seam control points used for Photo 14 of the Portland orthophotoquad. The resulting triangulation network is depicted in Figure 3b. Because direct application of this faceted surface is far too inefficient and computer-time-consuming for large data sets, the faceted surface is gridded or sampled by placing an evenly spaced rectangular grid over the surface to reduce the computation time and optimize computer resources during image resampling (Zobrist, 1982).

During the resampling process, the input image space is mapped into the output image space. At each grid intersection this mapping is exact; at other locations bilinear interpolation within the grid cell is used to locate the input pixel. Currently, a cubic convolution resampling algorithm is used for calculating the output pixel value. An assessment of the geometric accuracy of the transformed images verified that the goal of maintaining the accuracy of the digital orthophotos was met. Table 2 shows the predicted and measured passpoint locations of photo 14 before and after image transformation for mosaicking.

RADIOMETRIC CORRECTION AND MOSAICKING OF RECTIFIED AERIAL PHOTOGRAPHS

After all geometric corrections were applied and the geometric accuracy verified, the images were radiometrically matched and mosaicked. Working two images at a time, brightness correction information was collected along the polygonal seam boundary of the add-on image. The average pixel value for 10- by 10-pixel windows centered about the seam control points was computed for the reference and the add-on image, and the information was stored in tabular form. The average brightness differences between the two images was calculated. The remaining brightness differences were modeled using the gridded finite element technique discussed above; however, during radiometric correction the surface reflects the brightness adjustment to be applied at each vertex of the resulting triangles. At each grid intersection the brightness mapping is exact; at other locations bilinear interpolation within the grid cell was used to approximate the brightness adjustment to be applied to the input pixel. The corrected add-on image was cut precisely according to the polygonal boundary defined, and the two images were

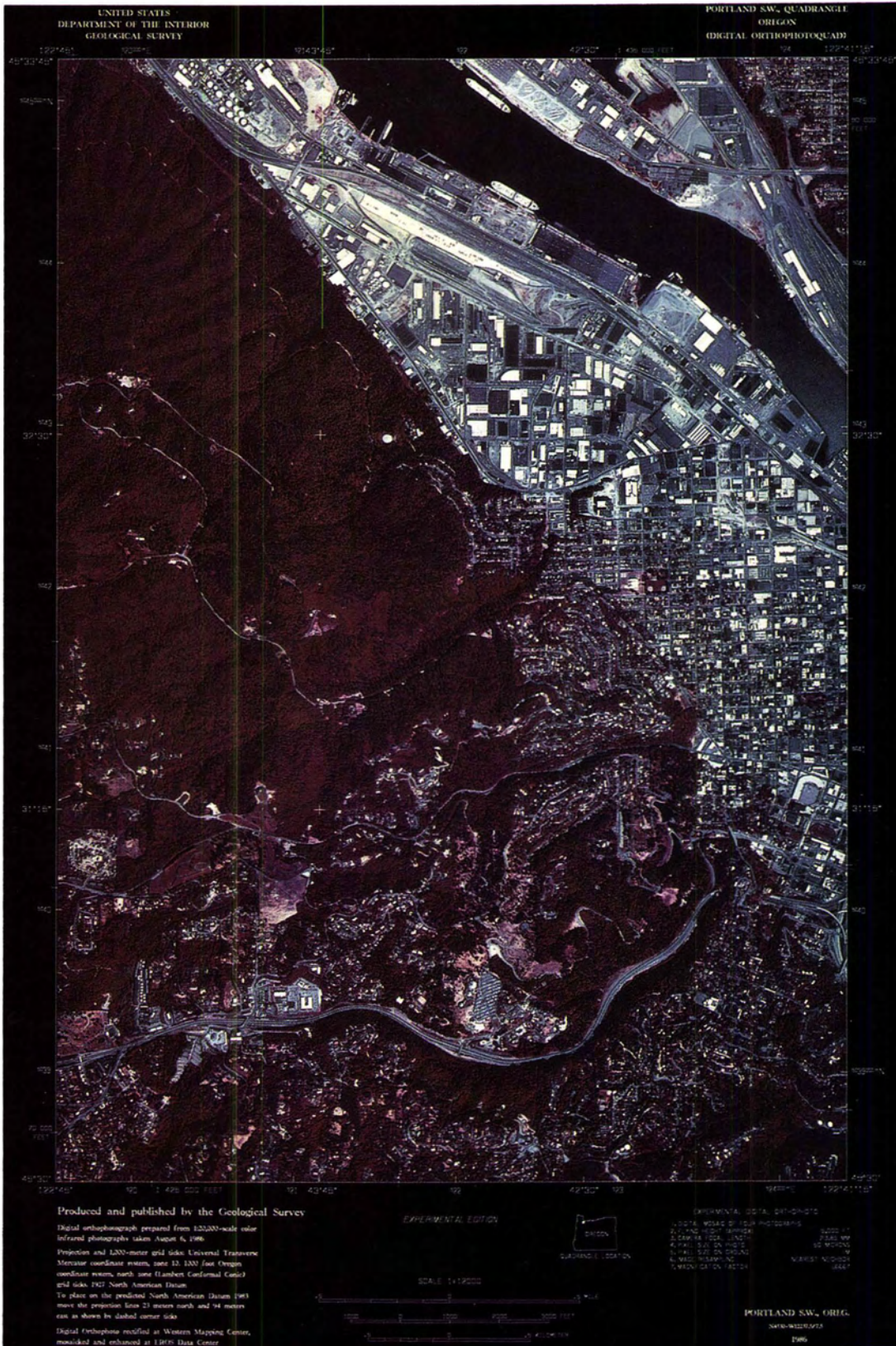


PLATE 1. Portland, Oreg. — Wash. S.W. Quarterquadangle.

mosaicked. The process was repeated for all subsequent images in the mosaic where the previously created mosaic was used for the brightness reference image. Brightness correction and mosaicking were repeated for all bands.

ENHANCEMENT OF DIGITAL ORTHOPHOTOS

To improve the appearance of the digital mosaic, enhancement techniques such as spatial filtering and contrast enhancement were applied to the image. A spatial filter was used to increase the effectiveness of the subsequent contrast enhancement process (Chavez, 1984). To increase the high-frequency component and sharpen the image, an edge enhancement was applied to the data (Chavez and Berlin, 1984). This edge enhancement was accomplished by applying a small kernel (3 by 3 or 5 by 5) spatial filter to the image to increase the high-frequency spatial variation, thereby increasing the radiometric differences between pixels along edges. After filtering, a multiple-point linear stretch was performed on each band. The cumulative histogram of each band was evaluated to determine the number and position of the breakpoints (Kidwell and McSweeney, 1984). The breakpoints were selected to provide a pleasing color product.

FUTURE RESEARCH

Additional research will be required to develop a digital orthophoto production system. Questions that must be answered include DEM resolution for specific orthophoto scales, optimum image resampling, format of the digital data, distribution media, and optimum output medium.

Currently, the standard 30-m spacing of DEM is used during the rectification process of 1:80,000-scale NHAP and a 1:40,000-scale NAPP images. For larger scale photography the 30-m cell spacing of the DEM is questionable. Continuing research will address the requirements for higher resolution DEMs.

Research has recently been completed to develop a modulation transfer function (MTF) deconvolution kernel for digitized aerial photography scanned on an Optronics C-4500 film scanner (Schowengerdt, 1988). The resulting kernel is then used in a table-lookup resampling algorithm to simultaneously restore and resample the processed imagery (Schowengerdt, 1988).

While the Optronics (essentially a whisk broom scanner) is similar to the Landsat MSS and TM and the AVHRR systems, operational differences dictated the decision to measure the MTF from special film targets scanned with standard instrument settings rather than attempting a detailed sensor model. Initial results suggest that MTF deconvolution can be applied to digitized aerial photographs, resulting in significant visual enhancement; however, the results are limited by film granularity and film tightness during scanning. Research will address the implementation of this work in the digital rectification process.

Research will be required to determine the media best suited for storing data sets the size of digital orthophotoquads (NAPP photography scanned at 50 micrometres results in approximately a 4,000 line by 4,000 sample image.) The Geological Survey is experimenting with storing the digital orthophoto in encoded format on a CD ROM. In addition, the issue of data format must be addressed. The digital orthophoto will require a header file containing such information as type of photography, geographic coverage, type and quality of DEM data used, date produced, and accuracy assessment information.

APPLICATIONS

Presently the Geological Survey is exploring the utility of large scale orthophoto products as a base map component of a local multipurpose cadastre for city, county, and regional agencies. Pilot projects of the Fontana, California, and Portland, Oregon, areas have been started. In the Fontana project, as well as pro-

ducing a 1:4,800-scale color infrared digital orthophoto, four 1:12,000-scale digital orthophotos were produced from 1:20,000-scale photographs. The four orthophotos were then digitally mosaicked to form a 1:24,000-scale orthophoto. In the Portland pilot project, 1:21,000-scale photographs were digitally rectified and mosaicked to create a 1:12,000-scale digital orthophoto (Plate 1). This orthophoto will be evaluated for use in field identification and classification, as well as for stereocompilation.

Other possible applications for digital orthophotoquads include map revision, custom maps, and as a base layer in a geographic information system (GIS) environment. Once contours have been captured for a quadrangle, incorporation of stereoinstruments in the mapping process is limited to the need to view new imagery in stereo for correct planimetric placement of new features. With the capability to produce digitized orthophotos, interpretation of new imagery can take place on image display devices rather than on a stereoplotter. New features could be captured in digital form directly and incorporated into the National Digital Cartographic Data Base. The capability to digitally rectify and mosaic aerial photographs makes the production of customized maps possible. Customized image processing techniques can be applied to enhance features of interest to various disciplines, such as geology, hydrology, and resource management. The digital orthophoto in a GIS environment can be overlaid with vector data, such as boundary, hydrography, and vegetation indexes, and can be used for a broad range of analysis.

CONCLUSIONS

The Geological Survey has developed the capability to produce digital orthophotos of high spatial resolution from scanned aerial photographs and DEM data. The accuracy is primarily limited by the quality of the DEM data used.

Once rectified, digital image processing techniques, such as mosaicking, contrast enhancement, and filtering, can be applied to improve the usefulness of the data. The capability to mosaic digital orthophotos provides the means to join not only images within a quadrangle but also to join adjacent quadrangles. Attention is being directed toward improving the efficiency of the techniques and designing a production system. Although much work remains, the digital orthophoto offers great potential to computer-aided cartography.

REFERENCES

- Chavez, P. S., 1984. Digital processing techniques for image mapping with Landsat TM and SPOT simulator data: *Proceedings of the 18th International Symposium on Remote Sensing of the Environment*, Paris, France, 1-5 October, pp. 101-116.
- Chavez, P. S., and G. L. Berlin, 1984. Digital processing of SPOT simulator and Landsat TM data for the SP Mountain Region, Arizona: *SPOT Simulation Applications Handbook, Proceedings of the 1984 SPOT Symposium*, Scottsdale, Arizona, 20-23 May, ASPRS, pp. 56-66.
- Horton, J., 1978. *The PDS Differential Rectifier: An Economical Approach to Digital Orthophotos*: Applied Optics Division, Perkin-Elmer Corp., Garden Grove, California, pp. 1-10.
- Keating, T.J., and D.R. Boston, 1979. Digital orthophoto production using scanning microdensitometers: *Photogrammetric Engineering and Remote Sensing*, Vol. 45, No. 6, pp. 735-740.
- Kidwell, R. D., and J. McSweeney, 1985. Art and science of image maps: *Proceedings of the 51st Annual ASP Meeting*, Vol. 2, Washington, D.C., 11-15 March pp. 770-782.
- Konecny, G., 1976. Mathematical models and procedures for the geometric restitution of remote sensing imagery: *Proceedings of Commission III of the XIII Congress of the International Society for Photogrammetry*, Helsinki, Finland, pp. 20-24.
- , 1979. Methods and possibilities for digital differential rectification: *Photogrammetric Engineering and Remote Sensing*, Vol. 45, No. 6, pp. 727-734.

Manacher, G. K., and A. L. Zobrist, 1978. A fast, space-efficient average-case algorithm for the "greedy" triangulation of a point set, and a proof that the greedy triangulation is not optimal: *Proceedings of the 16th Annual Allerton Conference on Communication, Control, and Computing*, Monticello, Illinois, 4-6 October, pp. 824-832.

Olsen, R., 1984. *Digital Orthophoto Concept*: Unpublished notes presented to technical staff, Western Mapping Center, U.S. Geological Survey.

Schowengerdt, R. A., 1988. *Research in Restoration of Digitized Aerial Photography*: Final Report to the EROS Data Center, Cooperative Agreement No. 14-08-0001-A-0330, University of Arizona, August.

Thormodsgard, June, and Thomas Lillesand, 1987. Comparison of the gridded finite element and the polynomial interpolations for geo-

metric rectification and mosaicking of Landsat data: *Proceedings of ASPRS-ACSM Annual Convention*, Vol. 2, Baltimore, Maryland, pp. 139-151.

Wolf, R., 1974. *Elements of Photogrammetry* (2d ed.): McGraw-Hill, Inc., New York, pp. 60-64.

———, 1982. Computation aspects of remapping digital imagery: *Proceedings of NASA Workshop on Registration and Rectification*, Leesburg, Virginia, 17-19 November, pp. 358-370.

Zobrist, A. L., N. A. Bryant, and R. G. McLeod, 1983. Technology for large digital mosaics of Landsat data: *Photogrammetric Engineering and Remote Sensing*, Vol. 49, pp. 1325-1335.

If You're a Member... Show You're Proud

Being a member of ASPRS has many privileges and one is this special membership certificate. Each member's name is engrossed in calligraphy - a symbol of pride, privilege and membership.

Yes, please order my certificate for \$8.00

Name (please print) _____

Name on certificate _____

Address _____

City/State _____

Zip Code _____ Telephone (_____) _____

Payment required with order:

Charge to: Visa or Mastercard

Card Expires _____ Mo./Yr.

Acct. No. _____

Signature _____

